Persistent Superconductivity in Ultrathin Pb Films: A Scanning Tunneling Spectroscopy Study

Daejin Eom,[1] S. Qin,[1] M.-Y. Chou,[2] and C. K. Shih[1]

[1]*Department of Physics and Center for Nano and Molecular Science and Technology, The University of Texas at Austin, Austin, Texas 78712, USA*

[2]*School of Physics, Georgia Institute of Technology, Atlanta, Georgia 30332, USA*

(Received 21 May 2005; published 18 January 2006)

By using a low temperature scanning tunneling microscope we have probed the superconducting energy gap of epitaxially grown Pb films as a function of the layer thickness in an ultrathin regime (5–18 ML). The layer-dependent energy gap and transition temperature (T_c) show persistent quantum oscillations down to the lowest thickness without any sign of suppression. Moreover, by comparison with the quantum-well states measured above T_c and the theoretical calculations, we found that the T_c oscillation correlates directly with the density of states oscillation at E_F. The oscillation is manifested by the phase matching of the Fermi wavelength and the layer thickness, resulting in a bilayer periodicity modulated by a longer wavelength quantum beat.

DOI: 10.1103/PhysRevLett.96.027005 PACS numbers: 74.78.Na, 73.21.Fg, 74.50.+r, 74.62.Yb

Thin film superconductivity is a subject of great scientific and technological importance. There are a few intriguing aspects for 2D superconductivity. One of them is the existence of a superconductor-insulator transition in thin films with disorder, where the onset of superconductivity is defined by a critical sheet resistance [1,2]. As the sheet resistance is inversely proportional to the thickness, it is found that the transition temperature (T_c) decreases rapidly in very thin films. This phenomenon has inspired tremendous scientific interests focusing on how fluctuations in the order parameter (both amplitude and phase) manifest themselves in ultrathin films and how such manifestations can lead to a superconductor-insulator transition [3]. Another aspect is the possible role of quantum confinement of single particle states upon the collective electronic phenomenon of superconductivity [4–9]. In 1963 Blatt *et al.* predicted resonances of the superconducting energy gap as a function of the thickness [4]. While early experimental studies on thin Sn films observed certain T_c oscillations [8], subsequent studies on many other metallic thin films did not exhibit such effects. Many attributed this inconsistency to the large number of defects in these thin films. Most recently, by using epitaxial thin Pb films, Guo *et al.* [9] reported the observation of T_c oscillations, albeit only a few periods, thus reopening the issue of quantum confinement effects on superconductivity. Unfortunately, the observed T_c oscillations are anticorrelated with the energy distribution of the quantum-well states (QWS) measured using photoemission spectroscopy. Moreover, as the measurements were performed using *ex situ* transport measurements after covering the film with a thin Au layer, it is unclear whether or not the measurements actually reflect the properties of thin Pb films. This study also reported a rapid decrease of T_c below 20 ML, similar to the universal behavior of T_c suppression as observed in disordered films at very thin thickness. This was interpreted again as the effect of quantum phase fluctuation which breaks the long range coherence of cooper pairs.

Here we report a direct probe of the superconducting gap of epitaxially grown crystalline Pb films in the ultrathin regime (5–18 ML) by using scanning tunneling microscopy/spectroscopy (STM/S). In contrast to previous studies using transport measurement, we find that the 2D Cooper pair condensates remain extremely robust down to the thinnest film (5 ML) without any signature of suppression. Moreover, we found very persistent quantum oscillations of superconductivity as a function of thickness even in this ultrathin regime. In addition, the oscillation correlates directly with the density of states (DOS) oscillation at E_F.

(111)-oriented Pb thin films are epitaxially grown on a Si(111) 7×7 surface in ultrahigh vacuum (UHV) and studied *in situ* using a home-built low temperature (LT) STM. Depending on the details of growth parameters, either globally flat films [LT deposition followed by room temperature (RT) annealing] or large 2D islands with flat-top geometry (a simple RT deposition) can be formed. For STM studies, it is convenient to use 2D islands since the local thickness referenced to the wetting layer can be unambiguously determined. A STM image of such an example is shown in Fig. 1(a) where the flat-top 2D island contains regions of 5, 6, and 7 ML height due to the substrate steps. The lateral width of these regions is of the order of 100 nm or larger while the vertical height is only slightly over 1 nm. The strong vertical confinement leads to the formation of QWS which are observable in tunneling spectra [Fig. 1(b)]. Also shown in Fig. 1(c) are the locations of QWS as a function of the thin film layer thickness, L (even layers are labeled red and odd layers blue), where the level spacing decreases as the L increases. One consequence of the L-dependent QWS is the apparent contrast of the STM image [10]. For example, Fig. 1(a), where the image is acquired at low bias, the 6 ML region shows brighter contrast than the 5 and 7 ML regions due to the fact that 6 ML has a QWS near E_F, while the QWS for 5 and 7 MLs are farther away from E_F [see Fig. 1(c)]. Oscillations of QWS near E_F are repeated from 8 to 14 MLs, except that the phase is

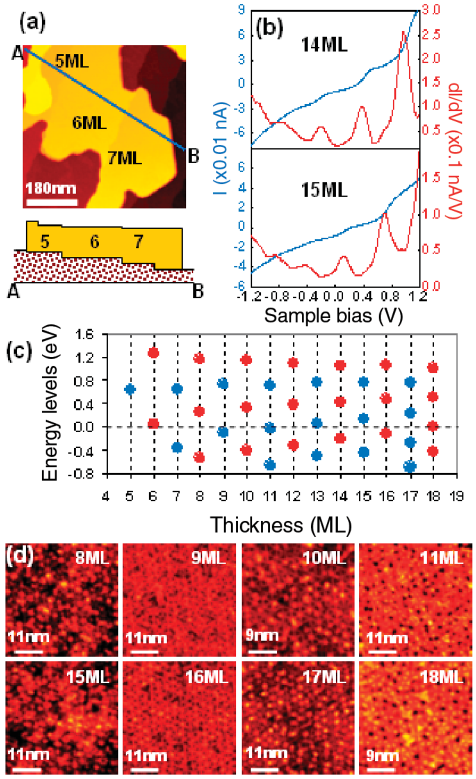

FIG. 1 (color). (a) A typical STM image of a Pb 2D island with a flat-top geometry containing regions of 5, 6, and 7 ML heights due to the substrate steps. This image was taken with sample bias, $V_{\mathrm{sample}} = +100$ mV, and tunneling set current $I_t = 100$ pA. Schematic of the cross section along the line AB in the STM image is shown below. (b) Tunneling current (blue) and differential conductance (red) spectra for 14 and 15 ML. The peak positions in the differential conductance spectra correspond to the locations of quantum-well states. (c) Display of the locations of quantum-well states for various thicknesses (5–18 ML). The red color is for even numbers of MLs and the blue is for odd numbers of MLs. (d) A series of STM images for several different thicknesses. They were all taken at 6.8 K with $V_{\mathrm{sample}} = +30$ mV and $I_t = 120$ pA.

reversed. Namely, the odd layers (labeled blue) have QWS close to E_F. After 15 ML, the situation reverses again where the even layers have QWS close to E_F. The origin of such oscillations of QWS near E_F can be understood because the Fermi wavelength, λ_F, of the bulk Pb band structure along the [111] direction, versus the spacing between (111) planes, t_0, is roughly 4:3; namely, $1.5\lambda_F \sim 2t_0$. This leads to a phase matching between λ_F and the vertical standing wavelength roughly every other layer. Nevertheless, the phase matching is not perfect and the accumulation of small phase errors eventually leads to a phase slip of the bilayer oscillations. This bilayer, plus 7 ML beating periodicity, can also be observed directly on the STM image fine structures shown in Fig. 1(d). The bilayer periodicity is reflected by the contrast reversal between even/odd layers from 8–11 ML. An almost identical contrast reversal between odd/even layers is found in the 15–18 ML range. This clearly shows a pattern repetition when the layer thickness differs by 7 ML.

It has been found that such QWS have profound effects on the thermodynamic stability of thin metal films in many sample systems [11–16]. The oscillation is characterized by a bilayer periodicity but phase modulated by a 9 ML periodicity in precisely the same way as the oscillatory QWS near E_F described here, except that we have observed a modulation periodicity of 7 ML instead of 9 ML reported earlier. This difference is likely due to the fact that the lattice constant at 4 K is 0.75% smaller than that at RT [17], causing faster accumulation of phase matching errors.

The superconducting gap is directly probed using scanning tunneling spectroscopy (STS) as a function of the temperature. Shown in Fig. 2(a) are normalized dI/dV vs V tunneling spectra acquired at various temperatures on a 10 ML region. The superconducting gap is clearly visible at 4.5 K and gradually disappears as the temperature is raised above 6.1 K. These spectra can be fitted with the BCS-like DOS [18] to obtain a temperature-dependent superconducting gap, $\Delta(T)$ [see Fig. 2(b)]. The Δ vs T data [Fig. 2(c)] can then be fitted with the BCS form to obtain both T_c (6.04 K) and Δ_0 (1.16 meV). The fitted

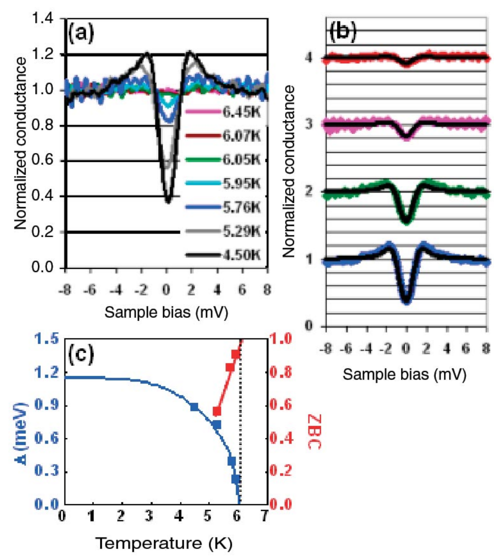

FIG. 2 (color). (a) A series of normalized conductance spectra for 10 ML with variation of temperatures. The normalized conductance was obtained by dividing every conductance spectrum by normal-state conductance data (i.e., 6.45 K data). (b) The normalized conductance spectra (nonblack colors) taken by STM were fitted using the BCS-like formula for the tunneling conductance (black). (c) The energy gaps Δ for several temperatures were obtained from Fig. 2(b) and plotted as blue squares. The blue curve is a fitting of these energy gap data using a BCS-like gap equation. From these fittings, we could determine $T_c = 6.04$ K and $\Delta_0 = \Delta(T = 0\ \mathrm{K}) = 1.16$ meV. The red squares are ZBC values of normalized conductance spectra at several temperatures and the red line is a linear fit to them. From the condition ZBC = 1, we could get $T_c = 6.09$ K, which is similar to the value obtained by the BCS-like gap equation.

value for T_c is consistent with the fact that when the sample temperature is raised to 6.1 K, the gap disappears completely. Certainly, the determination of Δ_0 and T_c using this procedure relies on whether or not $\Delta(T)$ has a BCS-like functional form. To provide an independent determination of T_c we note that if we use the tunneling spectra acquired near T_c (say within 1 K), the zero bias conductivity (ZBC) shows linear dependence with respect to the temperature. This observation allows us to simply extrapolate T_c as the point where ZBC = 1. Using this simple *parameter free* scheme, we found a T_c of 6.09 K, consistent with the value of 6.04 K using the more elaborate fitting scheme described above.

The layer-dependence of the superconducting energy gap is also probed. Shown in Fig. 3(a) are temperature-dependent spectra acquired on 5, 6, and 7 ML regions, respectively. At all temperatures below T_c, one observes that the gap in 6 ML is always larger than the gaps in 5 and 7 ML, reflected by the lower ZBC values in the spectra for 6 ML at all temperatures. The fitted values for $\Delta(T)$ are shown in Fig. 3(b). The same fitting procedure results in T_c values of 6.09, 6.31, and 6.14 K for 5, 6, and 7 ML, respectively. This difference in T_c is also evident by examining directly the spectra at 6.24 K when the gap in 6 ML is clearly observable but totally disappears in 5 and 7 MLs. We note that the precision for T_c determination is subjected to some uncertainties depending on the temperature calibration and the functional form of Δ vs T and can be as large as 0.1 or 0.2 K. However, since all these regions are probed within the same time frame, ensuring that they are measured at an *identical* temperature, the determination of the relative strength of the energy gap cannot be mistaken.

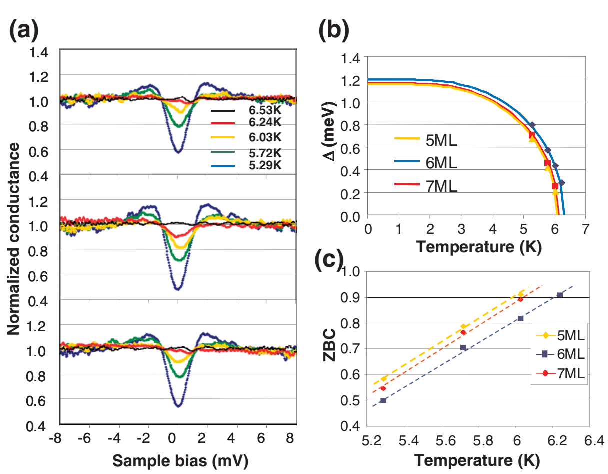

FIG. 3 (color). (a) Temperature-dependent variation of normalized conductance spectra for 5, 6, and 7 ML, respectively. (b) The extracted energy gaps from the normalized conductance spectra (discrete symbols) and relevant fittings of BCS-like gap equations (curves) for 5, 6, and 7 ML. T_c is determined from the fittings as 6.09, 6.31, and 6.14 K for 5, 6, and 7 ML, respectively. (c) ZBC values of normalized conductance at different temperatures illustrating the layer-dependent contrast of the energy gap at all temperatures.

This can also be clearly seen in the contrast of the ZBC values shown in Fig. 3(c). Thus, even though the absolute T_c is subjected to systematic errors, the relative change in T_c versus layer thickness can be accurately determined.

Shown in Fig. 4(a) is T_c vs L determined from temperature-dependent gap measurements following similar procedures, where the oscillatory behavior of T_c is quite evident. We note that a straightforward extrapolation of the ZBC of T_c vs L, gives identical oscillatory behavior except that the absolute values of T_c's are offset higher by roughly 0.05 K. Also shown in Fig. 4(b) is the DOS (E_F) estimated using a simple infinite well model for free standing Pb film as a function of the layer thickness. The Pb-Si interface generates a unique phase shift for the confined electrons, giving rise to an effective overall phase change in any thickness-dependent oscillation curve. To correct for this effect, we line up the positions of QWS with those determined experimentally [Fig. 4(c), same as Fig. 1(c)] and the shifted curve is shown in Fig. 4(b).

The layer-dependent T_c shows an oscillation amplitude of 0.25 K (~4%) between 5 to 8 ML and decay to an amplitude of about 0.1 K (1.5%) at larger thickness. On the other hand, the DOS (E_F) shows an oscillation amplitude of 12% at small thickness and then decay to about 4% at larger thickness. Thus, except for a reduction of quantum oscillation amplitude of a factor of 3, the T_c oscillations show good agreement with the DOS oscillations. In particular, the locations where phase slip of bilayer oscillation occurs [i.e., the transition from odd (even) to even (odd) oscillation] are reproduced. The average T_c for these single crystal 2D films, however, is about 15% lower than the bulk T_c. Note that the DOS is only one factor that could contribute to superconductivity. Another factor, the electron-phonon interaction, may also exhibit the oscillatory quantum size effect [19]. If one takes the fitted value of Δ_0 for a different thickness, one finds that Δ_0 oscillates the same way as T_c does, resulting in a constant value of $2\Delta_0/k_B T_c$, similar to the bulk value of about 4.4.

It is amazing that the quantum oscillation of superconductivity persists in all the thicknesses that we have studied without any sign of suppression, in particular, in the ultrathin regime where previous studies all showed a quenching of superconductivity [9,20,21]. While the T_c oscillation was predicted as far back as 1963 (4) and experimental observations had also been reported [8,9], our work is the first to establish a direct correlation between T_c and DOS (E_F) oscillations. Recent work of Guo *et al.* actually showed anticorrelation between T_c and DOS (E_F) observed by photoemission [9], an inconsistency most likely due to the proximity effect of the Au overlayer. Their reported quenching of T_c below 18 ML is also likely a consequence of their inability to maintain long range film uniformity. It is interesting to note that all these quantum oscillation phenomena, be it the single particle states, the collective electronic properties, and even the thermodynamic stability in metallic thin films, are all manifested by the phase matching of the layer thickness ($2L$) and λ_F of the bulk

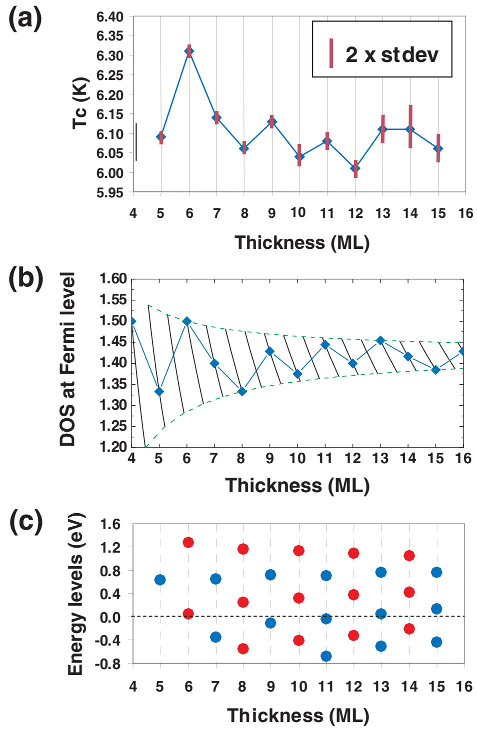

FIG. 4 (color). (a) A variation of critical temperatures T_c determined from temperature-dependent gap measurements for 5–15 ML. The estimation of the error bar is based on the estimation of the error bar in the determination of a ZBC value. Since, near T_c, ZBC can be approximated by a linear function, $\mathrm{ZBC}(T) \sim A(T - T_c) + 1$ with $A = 0.55\ \mathrm{K}^{-1}$, error bars in the determination of ZBC values, δ_{ZBC}, directly reflect the error bar in the determination of the relative change of T_c value, δT_c, through a simple relationship of $\delta T_c = \delta_{\mathrm{ZBC}}/A$. Statistical distribution of ZBC values determined from different tunneling measurements of the same layer thickness is used to determine δ_{ZBC}. (b) The calculated density of states near a Fermi level DOS (E_{F}) as a function of the layer thickness by using a simple infinite well model for free standing Pb film. To correct the phase shift at the surface and interface, a lineup of the positions of QWS with those determined experimentally is made. (c) The positions of QWS determined experimentally [the same as Fig. 1(c)].

band structure along the vertical direction, resulting in quantum oscillations with not only the bilayer periodicity but also a longer wavelength beating periodicity.

We note that our samples are epitaxial single crystal layer with uniform thickness over a lateral length scale of ~100 nm, longer than the coherent length. Thus, while the pairing along the vertical direction is completed quenched, the lateral pairing is completely unimpeded. Still, it is remarkable that such pairings are totally uninfluenced by scattering at the Pb/Si interface. It remains an open question whether or not the robustness of the 2D Cooper pair condensates and the quantum oscillation phenomenon can be maintained down to 1 or 2 ML, a question to be answered when single monolayer epitaxy can be achieved.

We further noticed that the T_c values (around 6 to 6.5 K) in our single crystal films are still about 15% lower than the bulk value of 7.2 K. Tunneling measurements on films up to 50 MLs show a similar T_c of around 6.2 K. On the other hand, measurements performed on 500 ML thick films indeed show the bulk value for T_c and the superconducting gap, suggesting the existence of a 3D to 2D transition thickness somewhere between 50 and 500 MLs. Most likely this transition would occur around the coherent length, a conjecture that should be verified by future experiments. It is also interesting that the constant value of $2\Delta_0/k_B T_c$ in these 2D films is the same as the bulk value despite a 15% difference in T_c. In an earlier experiment by Dyne *et al.* [21] on amorphous thin Pb films, it was also found that $2\Delta_0/k_B T_c$ remains constant despite a large variation of T_c from 1 to 7.2 K. It might suggest something fundamental related to the electron-phonon coupling in this material whose nature is yet to be unraveled.

Work supported by the National Science Foundation, DMR-0210383 and DMR-0306239.

[1] M. Strongin, R. S. Thompson, O. F. Kammerer, and J. E. Crow, Phys. Rev. B **1**, 1078 (1970).
[2] D. B. Haviland, Y. Liu, and A. M. Goldman, Phys. Rev. Lett. **62**, 2180 (1989).
[3] B. G. Orr, H. M. Jaeger, and A. M. Goldman, Phys. Rev. B **32**, 7586 (1985).
[4] J. M. Blatt and C. J. Thompson, Phys. Rev. Lett. **10**, 332 (1963).
[5] C. J. Thompson and J. M. Blatt, Phys. Lett. **5**, 6 (1963).
[6] A. Paskin and A. D. Singh, Phys. Rev. **140**, A1965 (1965).
[7] M. Yu, M. Strongin, and A. Paskin, Phys. Rev. B **14**, 996 (1976).
[8] B. G. Orr, H. M. Jaeger, and A. M. Goldman, Phys. Rev. Lett. **53**, 2046 (1984).
[9] Y. Guo *et al.*, Science **306**, 1915 (2004).
[10] I. B. Altfeder, K. A. Matveev, and D. M. Chen, Phys. Rev. Lett. **78**, 2815 (1997).
[11] A. R. Smith *et al.*, Science **273**, 226 (1996).
[12] Z. Zhang, Q. Niu, and C. K. Shih, Phys. Rev. Lett. **80**, 5381 (1998).
[13] V. Yeh, L. Berbil-Bautista, C. Z. Wang, K. M. Ho, and M. C. Tringides, Phys. Rev. Lett. **85**, 5158 (2000).
[14] W. B. Su *et al.*, Phys. Rev. Lett. **86**, 5116 (2001).
[15] D.-A. Luh, T. Miller, J. J. Paggel, M. Y. Chou, and T.-C. Chiang, Science **292**, 1131 (2001).
[16] P. Czoschke, Hawoong Hong, L. Basile, and T.-C. Chiang, Phys. Rev. Lett. **93**, 036103 (2004).
[17] *Thermophysical Properties of Matter*, edited by Y. S. Touloukian *et al.* (IFI/Plenum, New York-Washington, 1975), Vol. 12.
[18] J. Bardeen, L. N. Cooper, and J. R. Schrieffer, Phys. Rev. **108**, 1175 (1957).
[19] D.-A. Luh, T. Miller, J. J. Paggel, and T.-C. Chiang, Phys. Rev. Lett. **88**, 256802 (2002).
[20] D. L. Miller, Phys. Rev. B **15**, 4180 (1977).
[21] R. C. Dynes, A. E. White, J. M. Graybeal, and J. P. Garno, Phys. Rev. Lett. **57**, 2195 (1986).